Sandia National Laboratories
Waste Isolation Pilot Plant

Uncertainty Analysis of Actinide Solubilities for the 2026 Compliance Recertification Application (CRA-2026)

Work Carried Out under Task 6 of the Analysis Plan for WIPP Near-Field Geochemical Process Modeling, AP 153, Rev. 1.
To be included in the AP-153 records package

Paul Domski Digitally signed by Paul Domski Date: 2025.03.13 08:05:15 -06'00'

Authentication

Author: Paul S. Domski, Org. 08882

Technical Reviewer: Sungtae Kim, Org. 08881

QA Reviewer: Shelly R. Nielsen, Org. 08883

Management Reviewer: Chammi Miller, Org. 08882

Information Only

This page intentionally left blank

Information Only

TABLE OF CONTENTS

1 INTRODUCTION 7

2 METHODS 12

3 RESULTS 17

3.1 An(IV) Solubility Model 17

3.2 An(III) Solubility Model 22

4 CONCLUSIONS 30

5 REFERENCES 31

Appendix A. An(IV) and An(III) Uncertainty Outputs 35

Appendix B. Kutahyali Aslani (2022) Dataset 42

Information Only

LIST OF FIGURES

Figure 1. Histogram for the RPPCR/CRA-2024 of the difference D = log10 Sm – log10 Sp for Th(IV). 20
Figure 2. CDF plot for RPPCR/CRA-2024 of the difference D = log10 Sm – log10 Sp for Th(IV). 20
Figure 3. Histogram for the RPPCR/CRA-2024 of the difference D = log10 Sm – log10 Sp An(III). 25
Figure 4. CDF plot for the RPPCR/CRA-2024 of the difference D = log10 Sm – log10 Sp for An(III). 26
Figure A - 1. Graph of the Altmaier et al. (2004) measured data and EQ3NR model response using the DATA0.FM6 database with ThO_2(am) as the solubility-controlling phase..... 36
Figure A - 2. Graph of the Herm et al. (2015) and Xiong et al. (2017) measured data and EQ3NR model response using the DATA0.FM6 database with $Am(OH)_3$(am) as the solubility-controlling phase. 38
Figure A - 3. Graph of the Hinz et al. (2015) measured data and EQ3NR model response using the DATA0.FM6 database with $Am(OH)_3$(am) as the solubility controlling phase..... 38
Figure A - 4. Graph of the Neck et al. (2009) measured data and EQ3NR model response using the DATA0.FM6 database with $Am(OH)_3$(am) as the solubility controlling phase..... 39
Figure A - 5. Graph of the Runde and Kim (1995) measured data and EQ3NR model response using the DATA0.FM6 database with $Am(OH)_3$(s) as the solubility-controlling phase..... 39
Figure A - 6. Graph of the Rao et al. (1999) measured data and EQ3NR model response using the DATA0.FM6 database with $NaAm(CO_3)_2.6H_2O$(cr) as the solubility-controlling phase. ... 40
Figure A - 7 Graph of the Kutahyali Aslani (2022) measured data and EQ3NR model response using the DATA0.FM6 database with $Am(OH)_3$ (am) and $Am(OH)_3$ (cr) as the solubility-controlling phase at pcH = 9.0. 41

Information Only

List of Tables

Table 1. Abbreviations, Acronyms, Initialisms, etc. 9
Table 2. Run-Control Information for the Calculations Carried Out for the Original Analysis... 16
Table 3. Statistical Properties of the Distribution of D = log10(Sm) – log10(Sp) for Th(IV) for CRA-2026 compared with the CRA-2019 DPA and RPPCR data (Domski, 2019a, and 2023, respectively). 21
Table 4. CDF of the Differences between Measured and Predicted Th(IV) Solubilities for CRA-2026 . This CDF Defines the Solubility Multiplier SOLVAR for the Oxidation-State IV Model Material SOLMOD4 in the WIPP PA Parameter Database. 21
Table 5. Experimental matrix of the included data from Kutahyali Aslani (2022). 23
Table 6. Statistical Properties of the Distribution of D = log10(Sm) – log10(Sp) for An(III) for CRA-2026 compared with the CRA-2019 DPA and RPPCR data (Domski, 2019a, and 2023, respectively). 26
Table 7. CDF of the Differences between the Measured and Predicted Nd(III) and Am(III) Solubilities for the CRA-2026 . This CDF Defines the Solubility Multiplier SOLVAR for the Oxidation-State III Model Material SOLMOD3 in the WIPP PA Parameter Database. 28

Table A - 1 Studies included in the An(IV) uncertainty distribution with their EQ3NR filenames and D values. 35
Table A - 2 Statistics of the D values for each study included in the An(IV) uncertainty distribution. 35
Table A - 3 Studies included in the An(III) uncertainty distribution with their EQ3/6 filenames and D values. 36
Table A - 4 Statistics of the D values for each study included in the An(III) uncertainty distribution. 37

Table B - 1 Provides the Nd(III) concentrations in molarity, the sample date, the matrix composition, and the sample pcH. 42

Information Only

This page intentionally left blank

Information Only

1 INTRODUCTION

The actinide solubility uncertainty analysis provides distributions of the solubility multiplier SOLVAR for the oxidation state +III and oxidation state +IV model material SOLMOD3 and SOLMOD4 for the baseline solubility values in the WIPP Performance Assessment (PA) Parameter Database for the 2026 Compliance Recertification Application (CRA-2026). This analysis builds upon the Replacement Panels Planned Change Request (RPPCR) actinide solubility uncertainty analysis (Domski, 2023a). These distributions were generated by applying the WIPP geochemical model to peer-reviewed independent laboratory experimental data that meet project specific criteria. The analysis involved calculating the difference, the "D" value, between the $\log_{10}$ of the measured data and the $\log_{10}$ of the data simulated using the WIPP model. The D values were utilized to construct empirical cumulative distribution functions (CDF) to be sampled by the PA code. Multiple studies for the An(III)[1] and a single study for the An(IV) model were included in this uncertainty analysis, and were utilized to build the oxidation-state specific uncertainty distributions.

We do not include U(VI) in our analysis [See Section 2.2.8 of AP-153, Revision 1 Brush et al. (2012) for a discussion of U(VI)]. Instead, the EPA specified (U.S. EPA, 2006) that an estimate of 1×10^{-3} M be used for the solubility of U(VI) (SOLMOD6) in Generic Weep Brine (GWB) (SOLSOH) and Energy Research and Development Administration (WIPP Well) 6 (ERDA-6) (SOLCOH). For CRA-2026 it is possible the values of SOLMOD6 values of SOLCOH and SOLSOH will be updated based on new laboratory data, however, that information was not available at the time of writing this report.

GWB is a synthetic brine representative of intergranular Salado Formation brines at or near the stratigraphic horizon of the repository (Krumhansl et al., 1991; Snider, 2003). ERDA-6 (Popielak et al., 1983) is a synthetic brine representative of fluids in brine reservoirs in the Castile Formation, which underlies the Salado Formation.

An(V) is not included in this analysis because PA does not sample the uncertainties in the solubilities of An(V) in view of the fact that releases of this element do not affect the long-term performance of the WIPP (Brush and Garner, 2005).

This analysis report documents the actinide uncertainty distributions for the CRA-2026, and is independent of the repository inventory. This uncertainty analysis uses the WIPP database for EQ3/6, DATA0.FM6, and the literature screening criteria of Domski and Nemer (2023) for choosing experimental studies.

The difference between the current uncertainty analysis and that documented in Domski (2023a), which was for the RPPCR, is a new literature search that was executed to identify pertinent An(III) and An(IV) solubility studies in the period of January 9, 2023 to January 10, 2025, the time between the data cutoff date for the RPPCR and the CRA-2026 data cutoff.

---

[1] The term An(-) is the general term used for actinide with the value in parenthesis denoting its oxidation state.

Information Only

The EQ3/6 software package, Version 8.0a, (Wolery and Jarek, 2003; Wolery, 2008; Wolery et al., 2010; Xiong, 2011a) is used for this analysis. The WIPP thermodynamic database (DB) DATA0.FM6 (Domski, 2023b) was used for this analysis and is a deviation from AP-153, Revision 1(Brush et al., 2012) which specifies DATA0.FM1 (Xiong, 2011b).

We conducted our analysis under Task 6 of AP-153, Rev. 1, the current analysis plan (AP) for WIPP near-field geochemical process modeling (Brush et al., 2012, Subsection 4.4). This analysis was performed using the same process described as that used through the submission of CRA-2014, and therefore is a deviation from AP-153, Rev. 1. Table 1 defines the abbreviations, acronyms, initialisms, etc., used in this report.

Information Only

Table 1. Abbreviations, Acronyms, Initialisms, etc.

Abbreviation, Acronym, or Initialism	Definition
Am, Am(III)	americium, americium in the +III oxidation state
am	amorphous
An(-)	general term used for actinide with the value in parenthesis denoting its oxidation state
AP	analysis plan
aq	aqueous (dissolved in an aqueous solution)
atm	atmosphere(s)
C, c	carbon, crystalline
Ca, Ca^{2+}	calcium, calcium ion
CAP	(SNL/WIPP QA) corrective action plan
CCA	Compliance Certification Application
CDF	cumulative distribution function
citrate	$(CH_2COO)_2C(OH)(COO)^{3-}$ or $(CH_2CO_2)_2C(OH)(CO_2)^{3-}$
Cl, Cl^-	chloride, chloride ion
ClO_4, ClO_4^-	perchlorate, perchlorate ion
Cm, Cm(III)	curium, curium in the +III oxidation state
CMS	(Sandia/WIPP software) Configuration Management System
CO_3, CO_3^{2-}	carbonate, carbonate ion
col	colloidal (suspended in an aqueous or other solution)
CPR	cellulosic, plastic and rubber (materials)
cr	crystalline
CRA-2004	the first WIPP Compliance Recertification Application, submitted to the EPA in March 2004
CRA-2009	the second WIPP Compliance Recertification Application, submitted to the EPA in March 2009
CRA-2014	the third WIPP Compliance Recertification Application, submitted to the EPA in March 2014
CRA-2019 DPA	The fourth WIPP Compliance Recertification Application, Deferred Performance Assessment submitted to the EPA in March 2019
CRA-2026	The fifth WIPP Compliance Recertification Application.
RPPCR	Replacement Panels Planned Change Request
D	the difference(s) between logs (base 10) of the measured and predicted actinide solubilities (Sm and Sp)
EPA	(U.S.) Environmental Protection Agency
EQ3/6	a geochemical software package for speciation and solubility calculations (EQ3NR) and reaction-path calculations (EQ6), Version 8.0a
ERDA-6	Energy Research and Development Administration (WIPP Well) 6, a synthetic brine representative of fluids in Castile brine reservoirs
f_{CO_2}	fugacity (similar to the partial pressure) of CO_2
FMT	Fracture-Matrix Transport, a geochemical speciation and solubility code
G-Seep	a naturally-occurring brine formerly collected from G Drift in the WIPP underground workings and used for laboratory and modeling studies
GWB	Generic Weep Brine, a synthetic brine representative of intergranular Salado brines

Information Only

Abbreviation, Acronym, or Initialism	Definition
H, H^+	hydrogen, hydrogen ion
HCO_3, HCO_3^-	bicarbonate, bicarbonate ion
I	ionic strength, defined by $I = ½ \times \Sigma_i(M_i \times z_i^2)$, in which M_i and z_i are the molarity and charge of species i
I/O	(EQ3/6) input and output files
K, K^+	potassium, potassium ion
LIB	Library
log	the common logarithm or logarithm (base 10)
M	molar, mol•dm^{-3}
m	molal, mol•kg^{-1}
mcr	microcrystalline
Mg, Mg^{2+}	magnesium, magnesium ion
mM	millimolar
N	bin number (see Section 2 for explanation)
Na, Na^+	sodium, sodium ion
Nd, Nd(III)	neodymium, neodymium in the +III oxidation state
NO_3, NO_3^-	nitrate, nitrate ion
Np, Np(IV), Np(V)	neptunium, neptunium in the +IV oxidation state , neptunium in the +V oxidation state
O	oxygen
OH, OH^-	hydroxide, hydroxide ion
P	probability
PA	performance assessment, may refer to both the PA code, and/or the WIPP PA group
PABC	(WIPP) Performance Assessment Baseline Calculations, carried out in 2005 and 2009
pcH	the negative log (base 10) of the molar concentration of H^+
p_{CO_2}	partial pressure (similar to the fugacity) of CO_2
pmH	the negative log (base 10) of the molal concentration of H^+
ppm	parts per million
pH	the negative log (base 10) of the activity of H^+
Pu, Pu(III), Pu(IV)	plutonium, plutonium in the +III oxidation state, plutonium in the +VI oxidation state
QA	quality assurance
R	gas constant
Rev.	Revision
S_m	measured solubility
S_p	predicted solubility
SNL	Sandia National Laboratories
SO_4, SO_4^{2-}	sulfate, sulfate ion
T	temperature
Th, Th(IV)	thorium, thorium in the +IV oxidation state
TIC	total inorganic C (the sum of the dissolved species of inorganic C)
U, U(IV), U(VI)	uranium, uranium in the +IV oxidation state, uranium in the +VI oxidation state
µm	micrometer

Information Only

Abbreviation, Acronym, or Initialism	Definition
whewellite	$CaC_2O_4 \bullet H_2O$
WIPP	Waste Isolation Pilot Plant
XRD	X-ray diffraction
Zr, Zr(IV)	zirconium, zirconium in the +IV oxidation state
μ^0, μ^0/RT	standard chemical potential, dimensionless standard chemical potential

Information Only

2 METHODS

The method employed in the actinide uncertainty analysis has been largely unchanged since the Compliance Certification Application (CCA) PA. At its core is the creation of empirical frequency distributions based on the difference between the base 10 logarithm of measured laboratory solubility data and solubility data simulated with the WIPP model. These differences are compiled and sorted for a number of studies and the cumulative probability is calculated. These CDFs are sampled by the PA code and used as multiplier for the baseline solubility values for performance assessment.

The current uncertainty analysis follows this procedure:

1. Identify potential laboratory solubility studies using internet search tools.
2. Screen laboratory studies by applying our screening criteria (see below).
3. Create EQ3/6 input files to emulate as closely as possible the laboratory studies screened in from Step 2.
4. Execute the EQ3/6 inputs using the DATA0.FM6 database and post process the outputs using the Excel macro GetEQData_v101f.xls, i.e., extract the pH and An(III) or An(IV) concentrations.
5. Calculate, D, the log base 10 differences between the measured data and the simulated data.
6. Combine the D values for all oxidation state specific studies, sort the D values, and prepare empirical cumulative distribution functions.
7. Document all of the above steps in an analysis report (this report).
8. Provide a memo(s) for PA which includes the distributions of the solubility multiplier SOLVAR for the oxidation state III and oxidation state IV model material SOLMOD3 and SOLMOD 4, respectively, in the WIPP PA Parameter Database for the CRA-2026 .

A new literature search was initiated for CRA-2026. This literature search was broader based than previous searches in accordance with G1 and G6 (see below) (Domski and Nemer, 2023). The literature search for CRA-2026 included the period between January 9, 2023 to January 10, 2025. The literature search was facilitated by use of: 1) Google Scholar (https://scholar.google.com/), to obtain journal articles and conference papers, and 2) OSTI, to obtain US government reports (i.e., the G2 criterion) (https://www.osti.gov).

The literature screening that was completed for CRA-2026 identified five potential experimental studies for the An(IV) actinides, however, a detailed examination of these studies revealed that none of them met all of the screening criteria (see below), and as such none were included in the current uncertainty analysis. The CRA-2026 An(IV) actinide uncertainty distribution is the same as that used for the RPPCR (Domski, 2023a).

The An(III) literature screening identified five potential solubility studies which required in-depth screening to determine its eligibility for the CRA-2026 uncertainty analysis. One study (Kutahyali Aslani, 2022) included data that met all of the screening criteria and provided additional solubility data to be included in the An(III) uncertainty distribution.

Information Only

The WIPP screening criteria are used to determine which literature/experimental studies are included in the actinide uncertainty analysis and are documented in Domski and Nemer (2023). The criteria were presented to, and accepted by the EPA at the September 25, 2022 technical exchange meeting. From Domski and Nemer (2023):

Applicability:
These screening criteria are applicable to the selection of experimental data from the scientific literature for the purpose of validating the WIPP actinide solubility model under conditions modeled in PA. In this context, it is necessary to differentiate the two types of data typically considered in modeling, training data and test data. Training Data are those data used to fit free parameters to a given model, e.g., laboratory measurements of solubility which are used to fit the log K of a specific mineral phase. These screening criteria are ***not*** *intended for use in selecting Training Data, or to fit free parameters to the WIPP actinide solubility model for inclusion in the thermodynamic database. These screening criteria are applicable only to the selection of Test Data. Test Data are those data used to validate the WIPP actinide solubility model. For example, solubility measurements taken from the literature are compared to those predicted by the model parameterized with the log K fitted with the Training Data. The Test Data (S_m – **S**olubility **m**easured) and the model predictions (S_s – **S**olubility **s**imulated) are used to calculate the difference, or D values as $D = \log_{10}(S_m) - \log_{10}(S_s)$. The D values are then used to create an empirical distribution of model-prediction errors, which are sampled in PA and added to the $\log_{10}$ of the baseline solubility values.*

The new screening criteria, G-1 through G-10, are listed below:
G1 – Time Frame: *Preference given to data from studies after January 1990 with the emphasis on the period between the closure date of the most recent recertification cycle and the current recertification cycle. The closure date for the literature search is set to 3-months before the required parameter feed to performance assessment for the current recertification cycle. Studies prior to 1990 may be acceptable, provided the experimental and analytical methods are provided and defensible, and satisfies the remainder of the criteria listed herein.*
G2 – Sources: *Include data from studies in peer-reviewed journals unpublished undergraduate/graduate theses or dissertations, national and international laboratories, and organizations (e.g., officially released reports from government and educational national and international laboratories.), as well as studies originating from industry.*
G3 – Type of Data: *Include only those studies that provide solubility data. Exclude studies that do not provide solubility data (e.g., studies of corrosion, leaching, sorption, or transport).*
G4 – Solvent and Composition: *Include only data from studies in which water was the solvent and the solution composition characterized; exclude studies in which no aqueous phase was present (e.g., solids, molten metal or salts, or pure organic liquids).*
G5 – Temperature and Pressure: *Include only data obtained from studies that were performed at atmospheric pressures and temperatures of 20 - 30°C.*
G6 – Use of Oxidation-State Analogs*: Include data from studies that contain actinides currently in the WIPP model, or their appropriate oxidation-state analogs.*
G7 – Phase Characterization and Thermodynamic Equilibrium: *Include data from studies with a well-characterized solubility-controlling solid (both the starting and final solid phases) for which solubility parameters are in the WIPP model. Characterization of the final phase(s) may be complicated due to the presence of low-crystallinity hydrated phases, which may not be easily*

Information Only

identified. Methods used for phase identification must be well documented and appropriate for the experimental conditions. The solution separation technique (i.e., dissolved from colloidal) must be well documented and appropriate for the experimental conditions. The experimental procedure should discuss solid-phase synthesis procedures, including descriptions of precursors (solids and solutions); and whether equilibrium (including meta-stability) was obtained. Determination of equilibrium typically includes demonstration of stable concentrations and/or chemical conditions as a function of time.

***G8 – Applicability**: Include data from studies in which the participating chemical components (i.e., aqueous species and solid phases that may affect actinide solubility) are included in the WIPP model. Exceptions include the use of non-participating cations and/or anions, or additional known and characterized dissolved elements that have been demonstrated to not strongly complex or effect the solubility of the actinide(s) of interest.*

***G9 – Repeatability and Reproducibility:** Include only data from studies in which: 1) The investigators provided a sufficient description of their experiments to allow the work to be repeated by a qualified investigator; and 2) sufficient experimental data are provided to allow computer simulation of the experiments.*

***G10 – WIPP-Relevant Conditions:** Include data from experimental studies carried out under conditions [e.g., pcH, ionic strength, and total inorganic carbon (TIC)] similar to those expected for WIPP, as designated by the Chemical Conditions Conceptual Model.*

Experimental studies/data included in the WIPP actinide uncertainty analysis must meet the following conditions:

Parameter ranges for G10 literature screening criteria.

G10 Conditions	
Ionic Strength (m)	$5.0 \le I \le 9.5$ m[2]
	$0.0 \le Mg \le 1.6$ M
	$0.0 \le Ca \le 0.5$ M
pcH	$8.5 \le pcH \le 10.7$
Total Inorganic Carbon	$TIC = 0.0 - 2.0 \times 10^{-2}$ M

The CRA-2026 An(III) and An(IV) actinide uncertainty distributions were constructed using the RPPCR (Domski, 2023a) distributions and adding new data as appropriate. In the case of the An(IV) distribution no new data were identified for CRA-2026 and the RPPCR distribution will be used. For CRA-2026 the RPPCR An(III) uncertainty distribution was updated with an additional six data points identified from the Kutahyali Aslani (2022) solubility study. The WIPP thermodynamic database, DATA0.FM6, which was used for the RPPCR was not updated for

---

[2] The WIPP brines are predominantly sodium – chloride type brines but include an array of other dissolved ionic species (e.g., K^+, Mg^{2+}, Ca^{2+}, SO_4^{2-}, HCO_3^-, $B(OH)_4^-$, and Br^-), and as such the G10 ionic strength range mainly reflects the Na - Cl predominance. However, in the scientific literature actinide/lanthanide solubility studies are typically performed in single electrolyte solutions, mainly NaCl, $MgCl_2$, and $CaCl_2$, therefore, it is necessary to set WIPP appropriate upper bounds on dissolved Mg and Ca in this criterion. Note that the Mg and Ca limits are applicable to both single and multi-electrolyte solutions, however, the lower limit of ionic strength (5.0 m) is not applicable to Mg and Ca single-electrolyte systems.

Information Only

CRA-2026, therefore, it was not necessary to rerun the EQ3/6 inputs which were used to generate the RPPCR distributions.

In the EQ3NR runs generated for the new Kutahyali Aslani (2022) data, the pcH was specified; the composition of the laboratory supporting solution was used as input, in molar units; and the radionuclide composition was calculated based on equilibrium with the solubility-controlling phase in the experiment. Because the data are reported in molarity, it was necessary to input the following EQ3 input parameters: total dissolved solids (tdspl), solution density (rho), and the aqueous-phase scale factor (scamas). These parameters are calculated based on the fluid composition in the MS-Excel spreadsheet "*Conc_density_calcs_CRA26_Uncert.xlsx*." This spreadsheet will be archived to the SNL/WIPP Records Center at "/data/cvs/CVSLIB/WIPP_EXTERNAL/ap153_files/CRA2026"..

Each of the EQ3/6 files for each of the laboratory studies were executed, and the resulting EQ3NR output files (*.3o), or EQ6 output files (*.6o) were post processed using the Excel macro GetEQData_v101f.xls (archived in the records package). The results for the An(III) and An(IV) are compiled in the spreadsheets *An(III)_CRA2026_Uncertainty.xlsx* and *AN(IV)_CRA2026_Uncertainty.xlsx*, respectively, both of which are archived in the records package. Each of the laboratory studies is saved on separate tabs that are clearly labeled. These two spreadsheets also contain the probability distributions and CDF and histogram plots.

The frequency distributions were generated from the differences (D) between the logs of the measured and predicted actinide solubilities (S_m and S_p, respectively), and displayed as histograms in Microsoft Excel spreadsheets using Excel's frequency function in this commercial spreadsheet software. One other deviation was implemented. AP153, Rev. 1 (Brush et al., 2012) specifies that histograms of the data will be produced by binning the data and implies that the data will be used in this form. Instead, a constructed cumulative-distribution function (CDF) was defined from the raw data rather than the binned histogram data.

Negative values of D indicate that the Th(IV) or Am(III) model implemented in EQ3/6 predicted a solubility greater than the corresponding measured value (overprediction of solubility by the model); positive values of D indicate that the model predicted a solubility less than the measured value (underprediction). The Excel files "*An(III)_CRA2026_Uncertainty.xlsx"* and "*AN(IV)_CRA2026_Uncertainty.xlsx*" contain spreadsheets with S_m or S_p values (or logs thereof), frequency distributions, and histograms for this analysis. The variable D is calculated via:

$$D = \log_{10}(S_m) - \log_{10}(S_p)$$

Where S_m is the measured solubility, and S_p is the predicted solubility.

We will submit electronic copies of the files "*An(III)_CRA2026_Uncertainty.xlsx"* and "*AN(IV)_CRA2026_Uncertainty.xlsx*" and all of the other spreadsheets to the archived file "*CRA2026_An-Uncert.ZIP"*, which is stored at "/data/cvs/CVSLIB/WIPP_EXTERNAL/ap153_files/CRA2026".

Information Only

In this analysis, DATA0.FM6 (Domski, 2023b) was used to perform calculations to construct the uncertainty distributions based on the data sets meeting the literature screening criteria of Domski and Nemer (2023). We follow the rounding rules of Gamsjäger et al. (2012) for the numbers in the CDFs generated in this analysis.

Table 2. Run-Control Information for the Calculations Carried Out for the Original Analysis.

Description or Title of File(s)	Location of File(s)
EQ3/6 Database DATA0.FM6	In zip file Uncertainty_ CRA2026.ZIP, /data/cvs/CVSLIB/WIPP_EXTERNAL/ap153_files/CRA2026
Excel macro GetEQData_v101f.xls	In zip file Uncertainty_ CRA2026.ZIP, /data/cvs/CVSLIB/WIPP_EXTERNAL/ap153_files/ CRA2026
EQ3/6 I/O files and Excel spreadsheets with input and extracted data	In zip file Uncertainty_CRA2026.ZIP, /data/cvs/CVSLIB/WIPP_EXTERNAL/ap153_files/ CRA2026

Information Only

3 RESULTS

This section provides the results of the CRA-2026 actinide solubility uncertainty analysis for An(IV) (Subsection 3.1) and An(III) (Subsection 3.2).

3.1 An(IV) Solubility Model

Literature Screening

A literature search was performed for the CRA-2026 to identify experimental studies for inclusion in the An(IV) uncertainty analysis. The literature search identified five potential studies, with no data points having met all the screening criteria. See below for a brief overview of each study.

An(IV) Studies Considered for the CRA-2026 Actinide Uncertainty Analysis

Five potential An(IV) experimental solubility studies were identified for possible inclusion in the An(IV) actinide uncertainty analysis for CRA-2026. These studies are discussed below.

Nisbet et al. (2022) examined the effect of carbonate ligands on Th(IV) solubility/transport via the formation of stable aqueous complexes in hydrothermal systems. This was accomplished by study of the solubility of Th in carbonate-bearing fluids relevant to natural systems (0.05–0.5 m $NaHCO_3/Na_2CO_3$; pH_T ~ 7.8–9.8) at elevated temperature (175–250 °C). This study was eliminated from inclusion because of criteria G5 – the study temperature is out of range. No further consideration was required.

Yan et al. (2024) presents an updated chemical, thermodynamic, and activity model for the U(IV) – Na – Mg – Ca – H – Cl – H_2O system. This study is not a laboratory solubility study, but rather an interpretation of published data from other authors. As such this study does not meet the G3 screening criteria. Solubility data from two studies, Rai et al. (1997) and Cevirim-Papaioannou et al. (2018) were used by Yan et al. (2024). The Rai et al. (1997) were eliminated from consideration by Domski (2023a), and the study of Cevirim-Papaioannou et al. (2018) is discussed below.

Kiefer et al. (2022) studied the influence of aging temperature (80 °C), time (1.0, 2.0, 4.5 and 5.5 months), and pH (pmH 3.0 and 12.8) on freshly precipitated amorphous-hydrated thorium oxide [ThO_2(am,hyd)] and the effect on the solubility of the resulting solids. The solid materials were characterized using several methods which included: 1) X-ray diffraction (XRD); 2) X-ray photoelectron spectroscopy (XPS) and scanning electron microscopy (SEM); and 3) Thermogravimetric analysis (TG) with differential thermal analysis (DTA). Selected solids were used in the solubility experiments at 22 °C in 0.1 M NaCl solutions with $2.3 \leq pmH \leq 7.0$ to assess any systematic solubility variations caused by the aging conditions. None of the data from this study met the G10 criterion and were, therefore, not included in the uncertainty analysis.

The study of Cevirim-Papaioannou et al. (2018) investigated the redox behavior of uranium in NaCl solutions (0.1 and 5.0 M) at $2.0 \leq pmH \leq 14.5$, 22 °C, and in the presence of reducing chemical systems (Sn(II), $Na_2S_2O_4$, Sn(II) + TiO_2, Sn(II) + Fe(0), Sn(II) + Fe_3O_4). The results of the study indicate that U(VI) is reduced to U(IV), both in the aqueous and solid phase, under the

Information Only

experimental chemical constraints. The results show that the solubility of the resulting solid agrees with that of amorphous-hydrated uranium oxide [UO_2(am, hyd)]. While this is an important paper none of the measured solubility data meet the conditions of the G10 screening criterion. None of the data measured in the 0.1 M NaCl matrix solutions met the G10 ionic strength criterion, and unfortunately, for the 5.0 M NaCl matrix solution none of the data met the G10 pH criterion. The data were either collected at pH < 8, or pH > 10.7 (see Figure 3 of Cevirim-Papaioannou et al., 2018).

Beam (2022) investigated the formation of An(III)/An(IV) silica colloids by performing undersaturation experiments with $Nd(OH)_3$(s) for An(III), and $U(OH)_4$(s) for An(IV) in 5.0 M NaCl solutions at 2.0 ≤ pmH ≤ 10.0 with and without 4.0 mM dissolved silica. The results showed that silica neither formed colloids nor affected the solubility[3] of An(III) or An(IV), for the experimental conditions. Beam (2022) does not state if the solid phase $U(OH)_4$(s) synthesized for these experiments was characterized either before or after the experiments per criterion G7, therefore, these data do not qualify for inclusion in the CRA-2026 uncertainty analysis.

The results of the An(IV) literature search for CRA-2026 did not find any additional experimental data to be included in the distribution which was used for the RPPCR (Domski, 2023a). Therefore, the An(IV) actinide uncertainty distribution documented in Domski (2023a) should be implemented by PA in the CRA-2026, and the reader is referred to Domski (2023a) for a discussion of the An(IV) uncertainty analysis as no further discussion will be provided in the current document.

[3] Beam (2022) states with regard to An(IV): "A slight increase in solubility occurs around pH 10 in the presence of silica, which is consistent with the formation of $An(OH)(H_3Si0_4)_3^{2-}$…"

Information Only

The An(IV) Uncertainty Analysis

There was no changes made to the RPPCR An(IV) actinide uncertainty distribution (Domski, 2023a) for CRA-2026. Therefore, the remainder of Section 3 is the same as the RPPCR An(IV) uncertainty analysis as documented in Domski (2023a).

This section describes the comparisons of experimentally measured An(IV) solubility and the solubilities predicted using the WIPP An(IV) speciation and solubility model included in the EQ3/6 thermodynamic database, DATA0.FM6. The EQ3/6 code was not executed for the CRA-2026 An(IV) uncertainty analysis because there has been no changes to the thermodynamic database, DATA0.FM6, and no new experimental data since the RPPCR.

Figure 1 provides the histogram and Figure 2 provides the empirical CDF for the comparisons of experimentally measured and predicted Th(IV) solubilities for CRA-2026. The current comparison includes a total of seven measured and predicted solubilities. Table 3 summarizes the statistical parameters of the current frequency distribution for CRA-2026 compared with the CRA-2019 DPA and the RPPCR.

Inspection of Figure 1 shows that the WIPP Th(IV) model, the EQ3/6 code, and the database, DATA0.FM6, overpredicted 5 ($D < 0$) of the 7 measured solubilities included in the current analysis and underpredicted 2 ($D > 0$). The mean and median values of the log of the sampled uncertainty factor used to adjust the baseline Th(IV) solubilities are -0.758 and -0.947, respectively (Table 3), and the mean and median values of the sampled uncertainty factor are $10^{-0.758} = 0.174$ and $10^{-0.947} = 0.113$. (The WIPP PA codes uses actinide solubilities that are the products of the baseline solubilities and the sampled uncertainty factors).

The sorted D-values and their cumulative probability values, i.e., cumulative distribution function (CDF) for Th(IV) for CRA-2026 are tabulated in Table 4 and are shown graphically in Figure 2. The PA code will use this CDF to define the solubility multiplier SOLVAR for the oxidation-state +IV model, material SOLMOD4 in the WIPP PA Parameter Database in response to the selected data sets for CRA-2026.

Table 3 provides the descriptive statistics for CRA-2026 An(IV) actinides and compares them to the CRA-2019 DPA (Domski, 2019a) and the RPPCR (Domski, 2023a) values. Appendix A provides a breakdown of D values by author and study the statistics for each data set, and plots of the measured experimental data compared to the EQ3NR modeled data.

Information Only

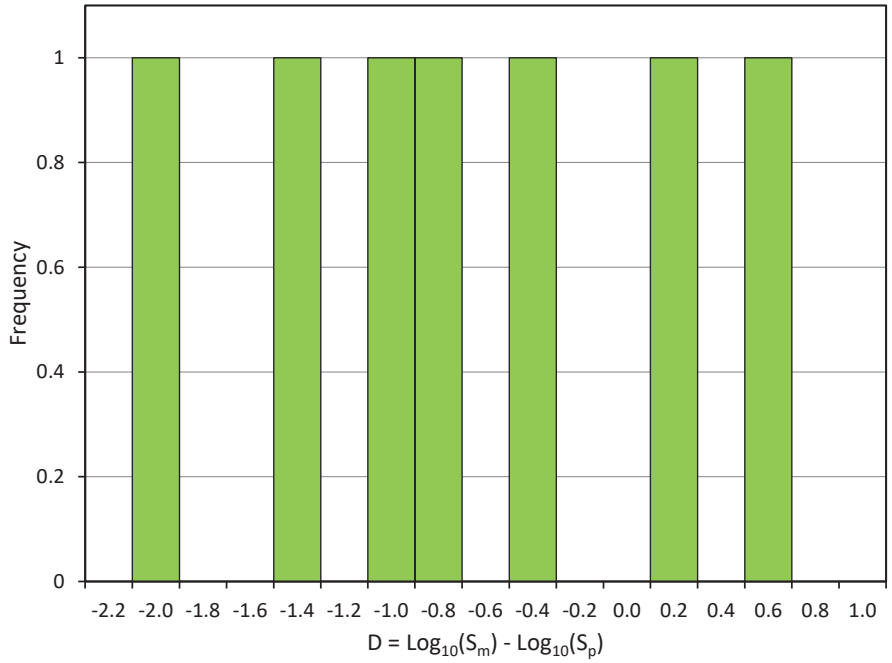


Figure 1. Histogram for CRA-2026 of the difference D = log10 Sm – log10 Sp for Th(IV).

Figure 2 is the An(IV) empirical CDF showing the D-values (-2.0 – 0.6) versus cumulative probability (0.0 – 1.0).

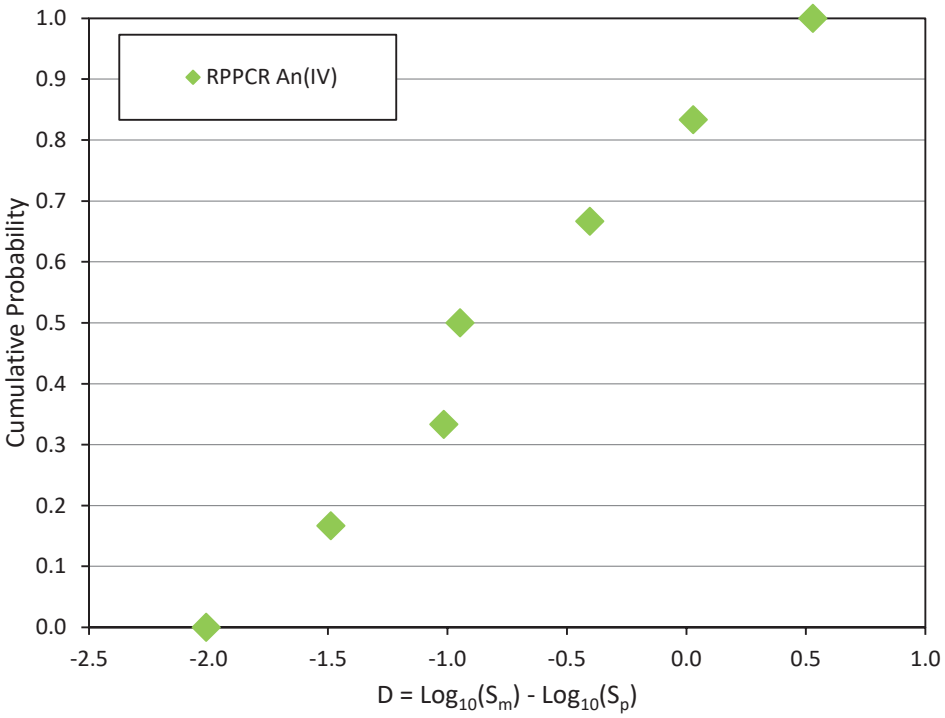


Figure 2. CDF plot for CRA-2026 of the difference D = log10 Sm – log10 Sp for Th(IV).

Information Only

Table 3. Statistical Properties of the Distribution of D = log10(Sm) – log10(Sp) for Th(IV) for CRA-2026 compared with the CRA-2019 DPA and RPPCR data (Domski, 2019a, and 2023a, respectively).

Analysis	Mean	Median	Standard Deviation	Minimum	Maximum
CRA-2019 DPA	–0.0114	–0.0900	0.821	–2.01	1.43
RPPCR	-0.758	-0.947	0.876	-2.01	0.53
CRA-2026	-0.758	-0.947	0.876	-2.01	0.53

There was no change to the CRA-2026 An(IV) uncertainty analysis from that of the RPPCR. The results of RPPCR and CRA-2026 uncertainty analysis show that the mean and maximum of the distribution is shifted to smaller (more negative in terms of the mean) values compared to the CRA-2019 DPA. The cause of the shift was the application of the update G10 criterion which eliminated data that was underpredicting the Th(IV) solubility. The Th(IV) model included in DATA0.FM6 is the same as that in the database used, DATA0.FM4 (Domski, 2019b), therefore, there was no impact of using the new database on the calculated Th(IV) concentrations. Table 4 provides the An(III) D-values and the cumulative probability values as shown I Figure 2.

Table 4. CDF of the Differences between Measured and Predicted Th(IV) Solubilities for CRA-2026 . This CDF Defines the Solubility Multiplier SOLVAR for the Oxidation-State IV Model Material SOLMOD4 in the WIPP PA Parameter Database.

D	*P(D<X)* for CRA-2026
-2.010	0.0000
-1.489	0.1667
-1.016	0.3333
-0.947	0.5000
-0.404	0.6667
0.029	0.8333
0.529	1.0000

Information Only

3.2 An(III) Solubility Model

Literature Screening

A new literature search was performed for CRA-2026 to identify experimental studies for inclusion in the CRA-2026 An(III) uncertainty analysis. The An(III) literature search included the following elements: Am(III), Nd(III), Cm(III), and Pu(III). The literature search identified five potential studies with all but one screened out, that of Kutahyali Aslani et al. (2022) which provided six additional data points to the An(III) uncertainty distribution. The five studies are discussed in detail below.

An(III) Studies Considered for CRA-2026 Actinide Uncertainty Analysis

The An(III) actinide empirical uncertainty distribution for CRA-2026 is an update to the RPPCR actinide uncertainty analysis (Domski, 2023a). For a discussion of the studies included in the RPPCR uncertainty analysis see Domski (2023a).

Five An(III) experimental solubility studies were identified for possible inclusion in CRA-2026 +III actinide uncertainty analysis and are discussed below.

Yang et al. (2023) investigated the americium solubility limiting solid phase for a proposed high-level radioactive site in China. This study was screened out by the G3 criterion because it was a modeling study and not an experimental study on the Am solubility limiting phase.

Kim and Cho (2022) studied the solubility of Am(III) in a synthetic groundwater using both modeling and laboratory experiments. The experiments were carried out from oversaturation using a synthetic water composition in the pH range of 7.5 – 10.0. Unfortunately, the ionic strength of the matrix solution was 1.5 mmol · kg^{-1} well below the 5 mol · kg^{-1} lower cutoff limit of the G10 criterion, therefore, this study was excluded.

Choi and Lee (2023) investigated the solubility of Nd(III) hydroxides in the pcH range of 6.5 – 10.5 in 0.1 M NaCl solutions. This study was eliminated based on the G10 ionic strength criterion.

Beam (2022) investigated the formation of An(III)/An(IV) silica colloids by performing undersaturation experiments with $Nd(OH)_3(s)$ for An(III), and $U(OH)_4(s)$ for An(IV) in 5.0 M NaCl solutions at $2.0 \leq pmH \leq 10.0$ with and without 4.0 mM dissolved silica. The results showed that silica neither formed colloids nor affected the solubility of An(III) or An(IV), for the experimental conditions. Beam (2022) provides an XRD trace of the $Nd(OH)_3$ starting material, however, he does not provide a discussion of the crystallinity of the sample used nor does he provide post-test solid phase characterization information. Neodymium hydroxide is known to occur both in the crystalline and amorphous states, each with different solubility products, therefore, per criterion G7 these data do not qualify for inclusion in the CRA-2026 uncertainty analysis.

Kutahyali Aslani (2022) investigated the effect of the organic ligands citrate and ethylenediaminetetraacetic acid (EDTA) on the solubility of neodymium hydroxide ($Nd(OH)_3$) in both the amorphous and crystalline form in two matrix solutions, 5 M NaCl and 90% GWB brine at pcH values of 7, 9, and 11. Six analytical results of Kutahyali Aslani (2022) met all of the

Information Only

screening criteria, Table 5 provides the experimental conditions for these data – the pcH and matrix solution composition, the $Nd(OH)_3(s)$ polymorph (amorphous or crystalline) and whether organic ligands were used in the experiment.

Table 5. Experimental matrix of the included data from Kutahyali Aslani (2022).

pcH	Solution	Phase	Organics
9.0	5 M NaCl	Amorphous	no
9.0	5 M NaCl	Amorphous	yes
9.0	5 M NaCl	Crystalline	no
9.0	5 M NaCl	Crystalline	yes
9.0	90% GWB[A]	Amorphous	no
9.0	90% GWB[A]	Amorphous	yes

A - Kutahyali Aslani (2022) did not run experiments in the 90% GWB using crystalline material.

Note, the 90% GWB composition used by Kutahyali Aslani (2022) included lithium ion (Li^+) at 3.9×10^{-03} mol L^{-1}. As a monovalent cation at low concentration it is expected that lithium complexation with EDTA and citrate would be negligible, and not affect the $Nd(OH)_3(s)$ solubility, or the solubility of any WIPP actinides. While Li^+ is not included in the WIPP thermodynamic database its presence in Kutahyali Aslani's experiments did not disqualify them from the current analysis.

This is the only study included in the An(III) uncertainty analysis which includes organic ligands and their impact on An(III) solubility. Both citrate and EDTA were added to the matrix solutions for the amorphous and crystalline phases as noted in Table 5. Unfortunately because they were added together it was not possible to discern their individual effect on Nd(III) solubility. The EQ3NR input files were set up according to the experimental constraints as listed in Kutahyali Aslani (2022). Kutahyali Aslani (2022) measured the Nd(III) concentrations at five times over course of the experiment, approximately at 33, 65, 97, 153, and 253 days[4], and the concentrations were relatively stable over all time periods. Therefore, the average Nd(III) concentrations for the sampling periods were used in this uncertainty analysis.

The An(III) Uncertainty Analysis

This section describes the comparisons of experimentally measured An(III) solubility and the solubilities predicted using the WIPP An(III) speciation and solubility model included in the EQ3/6 thermodynamic database, DATA0.FM6.

The following studies were included in CRA-2026 An(III) actinide uncertainty analysis, for a discussion of each study, 1 – 6 below, see Domski (2019a) and Knerr (2021). The study of Kutahyali Aslani (2022) is discussed above.

[4] The dataset from this study was requested from author, which included the sample time and concentration for the experimental matrix, these data are provided in Appendix B.

Information Only

1) One result from Xiong et al. (2017) in 5.0 M NaCl using $Am(OH)_3(am)$ as the solubility-controlling phase in DATA0.FM6.
2) Two results in 5.61 molal NaCl, and one result in 1.04 molal $MgCl_2$, for a total of three samples from Herm et al. (2015) using $Am(OH)_3(am)$ as the solubility-controlling phase in DATA0.FM6.
3) Five results from Hinz et al. (2015), two in 5.0 M NaCl 0.004 M $[B]_{tot}$, one in 0.25 $MgCl_2$ 0.004 M $[B]_{tot}$, one in 0.25 M $MgCl_2$ 0.04 M $[B]_{tot}$, and one in 1.0 M $MgCl_2$ 0.004 M $[B]_{tot}$. All using $Am(OH)_3(am)$ as the solubility-controlling phase in DATA0.FM6. There are two fewer results included in the current analysis than documented in the analysis of Domski and Nemer (2023) because replicate samples were combined and averaged.
4) Eleven results in ERDA-6 ($logP_{CO2(g)} = -3.5$) from Rao et al. (1999), were included in this analysis using $NaAm(CO_3)_2.6H_2O(cr)$ as the solubility controlling phase.
5) Five samples in 1.02 m $MgCl_2$ from Neck et al. (2009). $Am(OH)_3(am)$ was used as the solubility-controlling phase in DATA0.FM6.
6) Five 5.0 M NaCl samples of Runde and Kim (1995) were included in this analysis using the FM6 solubility-controlling phase $Am(OH)_3(s)$.
7) Six measurements from Kutahyali Aslani (2022) were included (see Table 5) three of which included the organic ligands citrate and EDTA.

Figures 3 and 4 provide the frequency histogram and the empirical CDF of the An(III) CRA-2026 D-values. The current comparison includes a total of 36 measured and predicted solubilities. Table 6 summarizes the statistical parameters of the current frequency distribution generated in this analysis with that of CRA-2019 DPA and the RPPRC (Domski, 2019a and 2023a, respectively).

Figure 3 shows that the WIPP Am(III) model, using DATA0.FM6 over predicted ($D < 0$) 25 of the 36 measured Nd(III) and Am(III) solubilities, and under predicted ($D > 0$) 11 of 36 experimental solubilities. The mean and median values of the log of the sampled uncertainty factor used to adjust the baseline Am(III) solubilities are -0.490 and -0.276, respectively (Table 6), and the mean and median values of the sampled uncertainty factor are $10^{-0.490} = 0.324$ and $10^{-0.276} = 0.530$. WIPP PA uses actinide solubilities that are the products of the baseline solubilities and the sampled uncertainty factors.

Table 7 provides values of the CDF for An(III) actinides for the CRA-2026, which are also graphically presented in Figure 4. PA will use this CDF to define the solubility multiplier SOLVAR for the oxidation-state III model, material SOLMOD3 in the WIPP PA Parameter Database for the PA calculations. Brush et al. (2005) described the PA implementation of these results in detail. Appendix A provides a breakdown of D values by author and study the statistics for each data set, and plots of the measured experimental data compared to the EQ3/6 modeled data. Figure 3 is a histogram of An(III) D-values, ranging from -2.75 to 0.75, versus frequency, 0.0 – 7.0.

Information Only

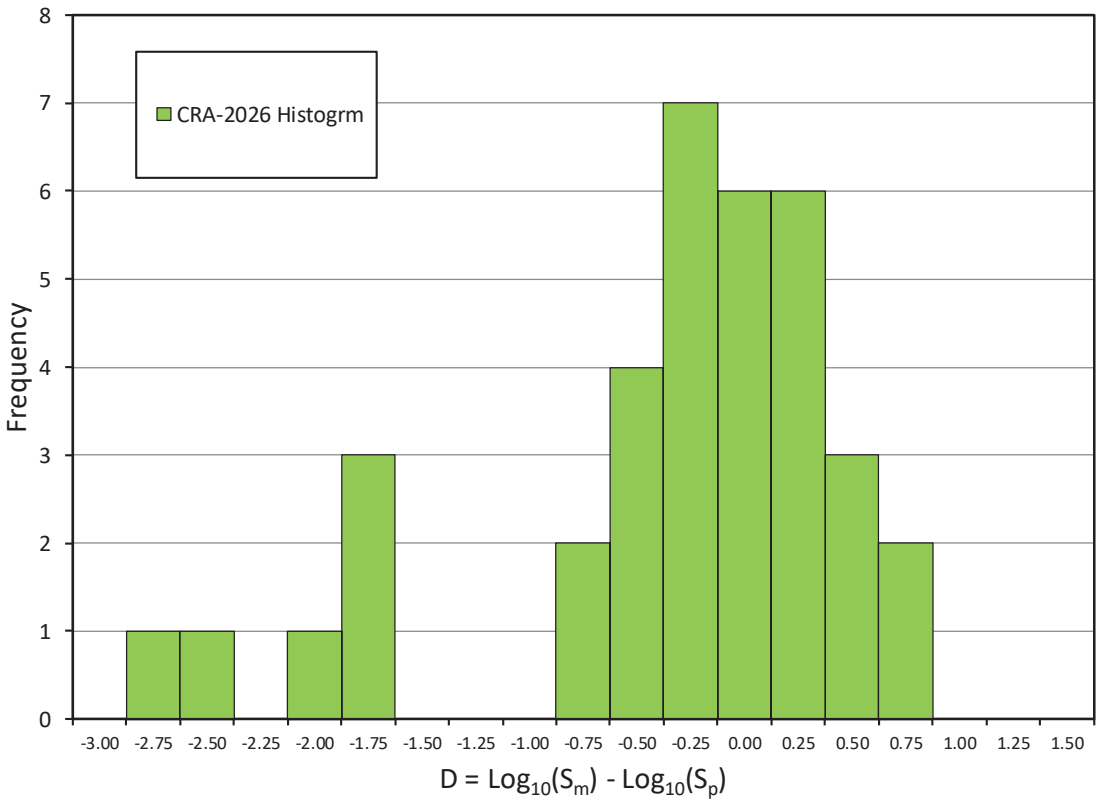


Figure 3. Histogram for the CRA-2026 of the difference D = log10 Sm – log10 Sp An(III).

Information Only

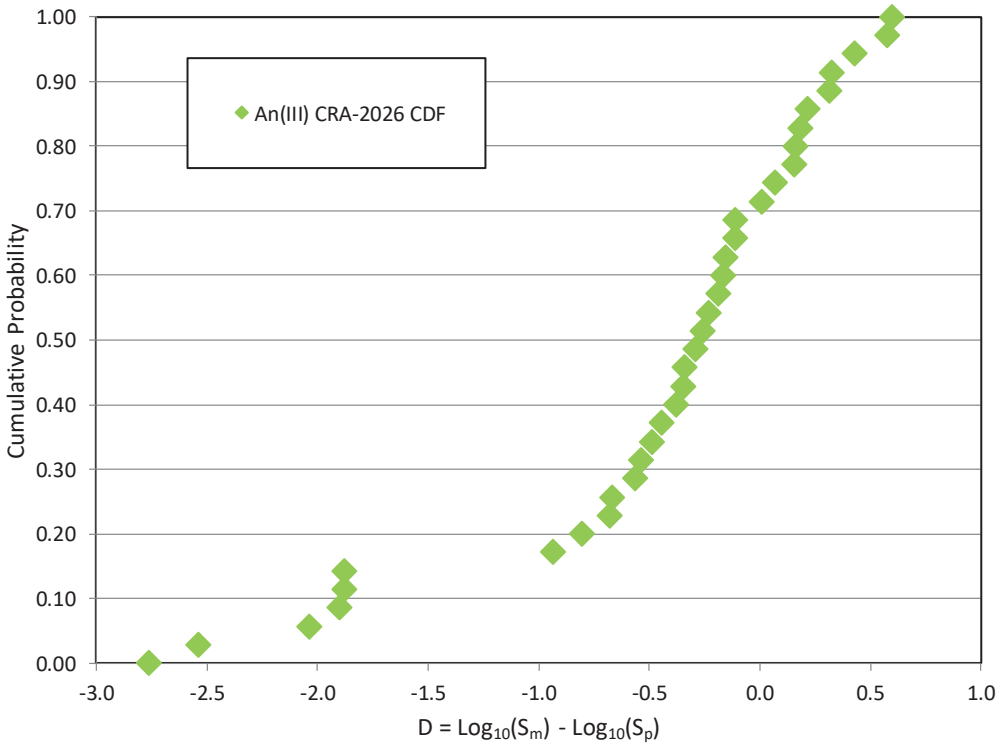


Figure 4. CDF plot for the CRA-2026 of the difference D = log10 Sm – log10 Sp for An(III).

Table 6. Statistical Properties of the Distribution of D = log10(Sm) – log10(Sp) for An(III) for CRA-2026 compared with the CRA-2019 DPA and RPPCR data (Domski, 2019a, and 2023a, respectively).

Analysis	Mean	Median	Standard Deviation	Minimum	Maximum
CRA-2019 DPA	0.651	0.516	1.01	-1.14	2.97
RPPCR	-0.509	-0.245	0.858	-2.76	0.578
CRA-2026	-0.490	-0.276	0.855	-2.76	0.598

Table 6 provides the mean, median, standard deviation, minimum, and maximum of the D-values for the An(III) actinides for the CRA-2019 DPA, the RPPCR, and the CRA-2026.

Compared to the CRA-2019 DPA results the RPPCR and CRA-2026 results are shifted to toward negative values. This is direct result of the use of the amorphous form of Am-hydroxide as the

Information Only

solubility-controlling phase which tends provide a better fit to the measured data, albeit the fits may tend to slightly over estimate the An(III) solubility resulting in small negative values.

Table 7 provides the An(III) D-values and the cumulative probability values as shown I Figure 4.

Information Only

Table 7. CDF of the Differences between the Measured and Predicted Nd(III) and Am(III) Solubilities for the CRA-2026 . This CDF Defines the Solubility Multiplier SOLVAR for the Oxidation-State III Model Material SOLMOD3 in the WIPP PA Parameter Database.

D	*P(D<X)* for CRA-2026
-2.76	0.0000
-2.54	0.0286
-2.034	0.0571
-1.90	0.0857
-1.88	0.1143
-1.88	0.1429
-0.932	0.1714
-0.806	0.2000
-0.678	0.2286
-0.666	0.2571
-0.563	0.2857
-0.536	0.3143
-0.488	0.3429
-0.443	0.3714
-0.379	0.4000
-0.343	0.4286
-0.341	0.4571
-0.292	0.4857
-0.260	0.5143
-0.229	0.5429
-0.185	0.5714
-0.164	0.6000
-0.155	0.6286
-0.113	0.6571
-0.112	0.6857
0.008	0.7143
0.068	0.7429
0.157	0.7714
0.161	0.8000
0.184	0.8286
0.215	0.8571
0.316	0.8857
0.327	0.9143
0.430	0.9429

Information Only

D	*P(D<X)* for CRA-2026
0.578	0.9714
0.598	1.0000

Information Only

4 CONCLUSIONS

The CRA-2026 actinide uncertainty analysis has been presented in this analysis report. This uncertainty analysis builds on the RPPCR (Domski, 2023a) analysis as both the RPPCR and the CRA-2026 uncertainty analysis used the DATA0.FM6 thermodynamic database (Domski, 2023b).

The literature screening identified five possible An(IV) solubility studies, none of which met all of the screening criteria. The results of the An(IV) CRA-2026, and RPPCR, uncertainty analysis showed that the mean and maximum of the distribution were shifted to smaller (more negative in terms of the mean) values relative to the CRA-2019 DPA. The cause of the shift was the application of the update G10 criterion for the RPPCR (Domski, 2023a) which eliminated data that was underpredicting the Th(IV) solubility, and not changes to the Th(IV) model. The Th(IV) model included in DATA0.FM6 is the same as that in the database used, DATA0.FM4 (Domski, 2019b), therefore, there was no impact of using the DATA0.FM6 database on the calculated Th(IV) concentrations.

Five potential solubility studies were identified for the CRA-2026 An(III) actinide uncertainty analysis. Data from one study, that Kutahyali Aslani (2022), met all of the screening criteria and provided additional data for the An(III) uncertainty analysis. Kutahyali Aslani (2022) investigated the effect of the organic ligands citrate and EDTA on the solubility if $Nd(OH)_3(s)$. For the first time the CRA-2026 An(III) actinide uncertainty analysis includes data, three measurements, which account for how the WIPP An(III)-organic model performs and contributes to An(III) solubility uncertainty.

Compared to the An(III) CRA-2019 DPA results the RPPCR and CRA-2026 results are shifted to toward negative values. This is direct result of the use of the amorphous form of Am-hydroxide as the solubility-controlling phase for some of the studies which tends provide a better fit to the measured data, albeit the fits may tend to slightly over estimate the An(III) solubility which leads to negative D values. The maximum of the An(III) uncertain distribution for the RPPCR/CRA-2026 was shifted by ~1 Log_{10} unit to the left compared to the CRA-2019 DPA while the minimum was unchanged.

Tables 4 and 7 provide values of the empirical CDFs for the An(IV) and An(III) actinides for the CRA-2026 PA, respectively.

Information Only

5 REFERENCES

Altmaier, M., V. Neck, and T. Fanghänel. 2004. "Solubility and Colloid Formation of Th(IV) in Concentrated NaCl and MgCl2 Solution," Radiochimica Acta. Vol. 92, 537 543.

Beam, J. C. (2022). Actinide (III/IV)-Silica Colloids in the WIPP (No. LA-UR-22-31798). Los Alamos National Laboratory (LANL), Los Alamos, NM (United States).

Brush, L.H., and J.W. Garner. 2005. "Additional Justification of the Insignificant Effect of Np on the Long-Term Performance of the WIPP." Memorandum to D.S. Kessel, February 1, 2005. Carlsbad, NM: Sandia National Laboratories. ERMS 538533.

Brush, L.H., J.W. Garner and E. Vugrin. 2005. "PA Implementation of Uncertainties Associated with Calculated Actinide Solubilities." Memorandum to D.S. Kessel, February 2, 2005. Carlsbad, NM: Sandia National Laboratories. ERMS 538537.

Brush, L.H., P.S. Domski, and Y.-L. Xiong. 2012. "Analysis Plan for WIPP Near-Field Geochemical Process Modeling." AP-153, Rev. 1, February 8, 2012. Carlsbad, NM: Sandia National Laboratories. ERMS 556960.

Çevirim-Papaioannou, N., Yalçıntaş, E., Gaona, X., Dardenne, K., Altmaier, M., & Geckeis, H. (2018). Redox chemistry of uranium in reducing, dilute to concentrated NaCl solutions. Applied geochemistry, 98, 286-300.

Domski, P. S. 2019a. Uncertainty Analysis of Actinide Solubilities for CRA 2019. Sandia National Laboratories, Carlsbad, New Mexico. ERMS 571179.

Domski, P.S. 2019b. "Official Release of the Qualified Pitzer Thermodynamic Database, DATA0.FM4, for EQ3/6 under AP-183, Revision 1. Carlsbad, NM: Sandia National Laboratories. ERMS 571051.

Domski, P.S. 2023a. "Uncertainty Analysis of Actinide Solubilities for the Replacement Panels Planned Change Request (RPPCR) Performance Assessment and the 2024 Compliance Recertification Application (CRA-2024)". Carlsbad, NM: Sandia National Laboratories. ERMS 579529

Domski, P.S. 2023b. "An Update to the WIPP EQ3/6 Database DATA0.FM1 with the Creation of DATA0.FM6". Carlsbad, NM: Sandia National Laboratories. ERMS 579370.

Domski, P.S. and M.B. Nemer. 2023. "Revised Literature Screening Criteria for the WIPP Actinide Solubility Uncertainty Analysis, Revision 1". Carlsbad, NM: Sandia National Laboratories. SAND2023-01264O.

Gamsjäger, H., Gajda, T., Sangster, J., Saxena, S.K., Voigt, W., 2012. Chemical Thermodynamics of Tin, Chemical Thermodynamics Volume 12, 610 pp, Elsevier, Amsterdam.

Information Only

Herm, M., Gaona, T. Rabung, D. Fellhauer, C. Crepin, K. Dardenne, M. Altmaier, H. Geckeis. (2015). "Solubility and spectroscopic study of An(III)/Ln(III) in dilute to concentrated Na-Mg-Ca-Cl-NO_3 solutions." Pure and Applied Chemistry 87(5): 487-502.

Hinz, K., M. Altmaier, X. Gaona, T. Rabung, D. Schild, M. Richmann, D. T. Reed, E. V. Alekseev, H. Geckeis. (2015). "Interaction of Nd(III) and Cm(III) with borate in dilute to concentrated alkaline NaCl, $MgCl_2$ and $CaCl_2$ solutions: solubility and TRLFS studies." New Journal of Chemistry 39(2): 849-859.

Krumhansl, J.L., K.M. Kimball, and C.L. Stein. 1991. *Intergranular Fluid Compositions from the Waste Isolation Pilot Plant (WIPP), Southeastern New Mexico*. SAND90-0584. Albuquerque, NM: Sandia National Laboratories.

Kiefer, C., T. Neill, N. Cevirim-Papaioannou, D. Schild, X. Gaona, T. Vitova, K. Dardenne, J. Rothe, M. Altmaier and H. Geckeis. (2022). Interlink Between Solubility, Structure, Surface and Thermodynamics in the ThO_2(s, hyd)–H_2O(l) System. Front. Chem. 10:1042709.doi: 10.3389/fchem.2022.1042709

Kim, H. K., and Cho, H. R. (2022). Evaluation of americium solubility in synthesized groundwater: geochemical modeling and experimental study at over-saturation conditions. Journal of Nuclear Fuel Cycle and Waste Technology (JNFCWT), 20(4), 399-410.

Knerr, M. 2021. Letter to Ms. Lee Ann B. Veal, Radiation Protection Division. Subject: Supplementary Information as Requested by U.S. Environmental Protection Agency During technical Exchange Meeting on June 22, 2020. Enclosure 1 Geochem Supplement – 1 for CRA 2019. July 8, 2021. U.S. Department of Energy, Carlsbad Field Office, Carlsbad, NM. Letter #21-0236.

Kutahyali Aslani, C. (2022). Solubility of An $(OH)_3$ am and An $(OH)_3$ cr in the presence of Citrate and EDTA (No. LA-UR-22-32478). Los Alamos National Laboratory (LANL), Los Alamos, NM (United States).

Neck, V., M. Altmaier, T. Rabung, J. Luetzenkirchen, and T. Fanghänel. 2009. "Thermodynamics of Trivalent Actinides and Neodymium in NaCl, $MgCl_2$, and $CaCl_2$ Solutions: Solubility, Hydrolysis, and Ternary Ca-M(III)-OH Complexes," *Pure and Applied Chemistry*. Vol., 81, no. 9, 1555—1568.

Nisbet, H., Migdisov, A. A., Williams-Jones, A. E., van Hinsberg, V. J., Xu, H., & Roback, R. (2022). The solubility of thorium in carbonate-bearing solutions at hydrothermal conditions. Geochimica et Cosmochimica Acta, 330, 80-92.

Popielak, R.S., R.L. Beauheim, S.R. Black, W.E. Coons, C.T. Ellingson and R.L. Olsen. 1983. *Brine Reservoirs in the Castile Formation, Waste Isolation Pilot Plant Project, Southeastern New Mexico*. TME 3153. Carlsbad, NM: U.S. Department of Energy WIPP Project Office.

Information Only

Choi, R. and J.-Y. Lee 2023. Solubility behavior and characterization of neodymium (III) trihydroxide solid phase. Abstract published online (https://inis.iaea.org/records/719a1-z9t14) by the International Atomic Energy Agency.

Rai, D., A. R. Felmy, S. M. Sterner, D. A. Moore, and M. J. Mason. 1997. The Solubility of Th(IV) and U(IV) Hydrous Oxides in Concentrated NaCl and MgCl2 Solutions. Radiochimica Acta. 79: 239-247.

Rao, L., D. Rai, A.R. Felmy, and C.F. Novak. 1999. "Solubility of $NaNd(CO_3)_2 \cdot 6H_2O$(c) in Mixed Electrolyte (Na-Cl-CO_3-HCO_3) and Synthetic Brine Solutions," *Actinide Speciation in High Ionic Strength Media: Experimental and Modeling Approaches to Predicting Actinide Speciation and Migration in the Subsurface. Proceedings of an American Chemical Society Symposium on Experimental and Modeling Studies of Actinide Speciation in Non-Ideal Systems, Held August 26-28, 1996, in Orlando, Florida*. Eds. D.T. Reed, S.B. Clark, and L. Rao. New York, NY: Kluwer Academic/Plenum Publishers. 153-169.

Runde, W., and J.I. Kim. 1995. *Untersuchungen der Übertragbarkeit von Labordaten natürliche Verhältnisse: Chemisches Verhalten von drei- und fünfwertigem Americium in salinen NaCl-Lösungen (Study of the Extrapolability of Laboratory Data to Natural Conditions: Chemical Behavior of Trivalent and Pentavalent Americium in Saline NaCl Solutions)*. RCM-01094. Munich, FRG: Institute for Radiochemistry, Technical University of Munich. ERMS 241862.

Snider, A.C. 2003. "Verification of the Definition of Generic Weep Brine and the Development of a Recipe for This Brine." Analysis report, April 8, 2003. Carlsbad, NM: Sandia National Laboratories. ERMS 527505.

U.S. EPA. 2006. "Technical Support Document for Section 194.24: Evaluation of the Compliance Recertification – Actinide Source Term and Culebra Dolomite Distribution Coefficient Values." EPA Air Docket A 98-49, Item II B1-3. Washington, DC: U.S. Environmental Protection Agency Office of Air and Radiation.

U.S. EPA. 2022. "Technical Support Document for Section 194.24: Evaluation of the Compliance Recertification – Actinide Source Term Gas Generation, Backfill Efficacy, Water Balance, And Culebra Dolomite Distribution Coefficient Values." EPA DOCKET: EPA-HQ-OAR-2019-0534. Washington, DC: U.S. Environmental Protection Agency Office of Air and Radiation.

Wolery, T.J. 2008. "Analysis Plan for EQ3/6 Analytical Studies." AP-140, Rev. 0, May 15, 2008, Carlsbad, NM: Sandia National Laboratories. ERMS 548930.

Wolery, T.W., and R.L. Jarek. 2003. "Software User's Manual: EQ3/6, Version 8.0." Software Document Number 10813-UM-8.0-00. Albuquerque, NM: Sandia National Laboratories.

Information Only

Wolery, T.J., Y.-L. Xiong, and J.J. Long. 2010. "Verification and Validation Plan/Validation Document for EQ3/6 Version 8.0a for Actinide Chemistry, Document Version 8.10." Carlsbad, NM: Sandia National laboratories. ERMS 550239.

Xiong, Y.-L., 2011a. "WIPP Verification and Validation Plan/Validation Document for EQ3/6 Version 8.0a for Actinide Chemistry, Revision 1. Supersedes ERMS 550239." May 12, 2011. Carlsbad, NM. Sandia National Laboratories. ERMS 555358.

Xiong, Y.-L. 2011b. "Release of EQ3/6 Database DATA0.FM1." E-mail to Jennifer Long, March 9, 2011. Carlsbad, NM: Sandia National Laboratories. ERMS 555152.

Xiong, Y, L. Kirkes and C. Marrs. 2017. Long-Term experimental determination of solubilities of micro-crystalline Nd(III) hydroxide in high ionic strength solutions: applications to nuclear waste management. Aquatic Geochemistry 23:359–375.

Yan, Y., N. Cevirim-Papaioannou, X. Gaona, D. Fellhauer, and M. Altmaier. 2024. Thermodynamic Description of U(IV) Solubility and Hydrolysis in Chloride Systems: Pitzer Activity Model for the System U^{4+}-Na^{+}-Mg^{2+}-Ca^{2+}-H^{+}-Cl^{-}-OH^{-}-H_2O(l). Applied Geochemistry 171:106091.

Yang, S., Li, Z., & Pan, P. (2023). Americium solubility and solubility limiting solid phase (SLSP) analysis in groundwater of Beishan, a proposed site for the disposal of high-level radioactive waste in China. Applied Geochemistry, 152, 105650.

Information Only

Appendix A. An(IV) and An(III) Uncertainty Outputs

Appendix A provides the statistics for each study included in the An(IV) and An(III) uncertainty distribution. Plots are provided of the measured data as they appear in their respective reports (i.e., some are in terms of pcH and others pmH) compared to the equivalent EQ3/6 WIPP model results.

The An(IV) uncertainty distribution included only a single reference, therefore the values are the same those found in Table 3.

Table A - 1 Studies included in the An(IV) uncertainty distribution with their EQ3NR filenames and D values.

Author	EQ3/6 Filename	D
Altmaier et al. (2004), Fig 2 NaCl 5 M	01Alt04.3o	-1.489
Altmaier et al. (2004), Fig 2 NaCl 5 M	02Alt04.3o	-0.404
Altmaier et al. (2004), Fig 2 NaCl 5 M	03Alt04.3o	-0.947
Altmaier et al. (2004), Fig 2 NaCl 5 M	04Alt04.3o	-2.010
Altmaier et al. (2004), Fig 2 NaCl 5 M	05Alt04.3o	-1.016
Altmaier et al. (2004), Tbl 2 MgCl2 0.25 M	11Alt04.3o	0.529
Altmaier et al. (2004), Tbl 2 MgCl2 0.25 M	12Alt04.3o	0.029

Table A - 2 Statistics of the D values for each study included in the An(IV) uncertainty distribution.

Reference	Maximum	Minimum	Mean	Median	n
Altmaier et al (2004)	0.529	-2.01	-0.758	-0.947	7

Information Only

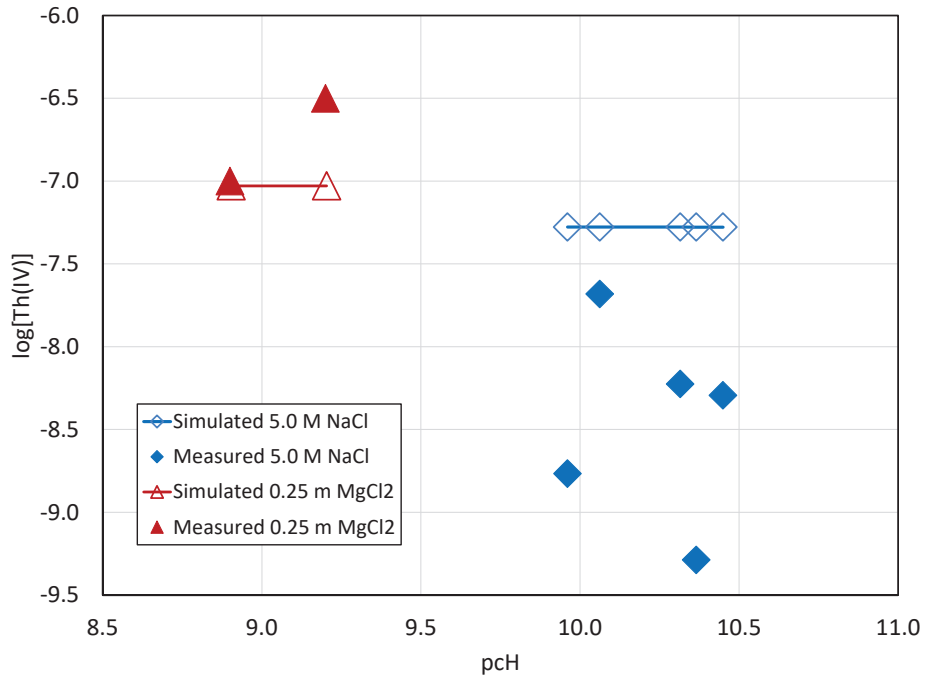


Figure A - 1. Graph of the Altmaier et al. (2004) measured data and EQ3NR model response using the DATA0.FM6 database with ThO_2(am) as the solubility-controlling phase.

Table A - 3 Studies included in the An(III) uncertainty distribution with their EQ3/6 filenames and D values.

Author	EQ3/6 Filename	D
Herm et al (2015) 1.04 m MgCl2	MgHerm1.3o	-0.343
Herm et al (2015) 5.61 m NaCl	NaHerm2.3o	-1.902
Herm et al (2015) 5.61 m NaCl	NaHerm3.3o	-2.536
Xiong et al., (2017) 5.0 m NaCl	Xio50ave.3o	-1.878
Hinz et al (2015) 5M NaCl, 0.004 Btot	NaHinz1.3o	-1.88
Hinz et al (2015) 5M NaCl, 0.004 Btot	NaHinz2.3o	-2.76
Hinz et al (2015) 0.25M MgCl2, 0.004 Btot	MgHinz1.3o	0.316
Hinz et al (2015) 0.25M MgCl2, 0.04 Btot	MgHinz1.3o	0.578
Hinz et al (2015) 1.0 M MgCl2, 0.004 Btot	MgHinz3.3o	-0.185
Neck et al. (2009) 1.04 m MgCl2	17NeckMg.3o	0.430
Neck et al. (2009) 1.04 m MgCl2	18NeckMg.3o	0.184
Neck et al. (2009) 1.04 m MgCl2	19NeckMg.3o	0.068
Neck et al. (2009) 1.04 m MgCl2	20NeckMg.3o	-0.155
Neck et al. (2009) 1.04 m MgCl2	21NeckMg.3o	-0.260
Runde & Kim (1995), 5 M NaCl	04Run95.3o	0.215
Runde & Kim (1995), 5 M NaCl	05Run95.3o	-0.443
Runde & Kim (1995), 5 M NaCl	06Run95.3o	-0.666
Runde & Kim (1995), 5 M NaCl	07Run95.3o	-0.488
Runde & Kim (1995), 5 M NaCl	08Run95.3o	-0.932
Rao et al. (1999), ERDA6, logpCO2=-3.5	05rao99.6o	-0.164
Rao et al. (1999), ERDA6, logpCO2=-3.5	06rao99.6o	-0.113
Rao et al. (1999), ERDA6, logpCO2=-3.5	07rao99.6o	0.157
Rao et al. (1999), ERDA6, logpCO2=-3.5	08rao99.6o	0.008
Rao et al. (1999), ERDA6, logpCO2=-3.5	09rao99.6o	-0.112

Information Only

Rao et al. (1999), ERDA6, logpCO2=-3.5	10rao99.6o	0.161
Rao et al. (1999), ERDA6, logpCO2=-3.5	11rao99.6o	-0.229
Rao et al. (1999), ERDA6, logpCO2=-3.5	12rao99.6o	-0.292
Rao et al. (1999), ERDA6, logpCO2=-3.5	13rao99.6o	-0.563
Rao et al. (1999), ERDA6, logpCO2=-3.5	14rao99.6o	-0.678
Rao et al. (1999), ERDA6, logpCO2=-3.5	15rao99.6o	-0.806
Aslani '22, Brine, amorphous, pcH9, no org	Br_am.3o	-0.379
Aslani '22,Brine, amorphous, pcH9, w/org	Br_am_or.3o	-0.536
Aslani '22,5M NaCl, amorphous, pcH9 no org	Na_am.3o	-2.034
Aslani '22,5M NaCl, amorphous, pcH9 w/org	Na_am_org.3o	-0.341
Aslani '22,5M NaCl, crystal, pcH9 no org	Na_cr.3o	0.327
Aslani '22,5M NaCl, crystal, pcH9 w/org	Na_cr_or.3o	0.598

Note: "Aslani '22" is shorthand for Kutahyali Aslani (2022).

Table A - 4 Statistics of the D values for each study included in the An(III) uncertainty distribution.

Reference	Maximum	Minimum	Mean	Median	n
Herm et al (2015)	-0.343	-2.54	-1.59	-1.90	3
Xiong et al., (2017)	-1.88	-1.88	-1.88	-1.88	1
Hinz et al 2015	0.578	-2.764	-0.787	-0.185	5
Neck 2009	0.430	-0.260	0.053	0.068	5
Runde & Kim (1995)	0.215	-0.932	-0.463	-0.488	5
Rao et al. (1999)	0.161	-0.806	-0.239	-0.164	11
Kutahyali Aslani (2022)	0.598	-2.034	-0.394	-0.360	6

Figures A – 2 – A – 7 present the An(III) simulated WIPP model fits using DATA0.FM6 to the measured experimental data that met the updated criteria (Domski and Nemer, 2023). For Figures A – 2 – A – 6 the Y-axis of each of these figures is the base 10 logarithm of the An(III) concentration, typically in the range of -9.0 to -4.0, and the X-axis is the pcH usually 8.0 – 11.0. Figure A – 7 also has the log base 10 of the An(III) as the Y-axis with the "count" as the X-axis, these data were measured at pcH = 9.0, therefore, a simple count of the data was used for plotting.

Information Only

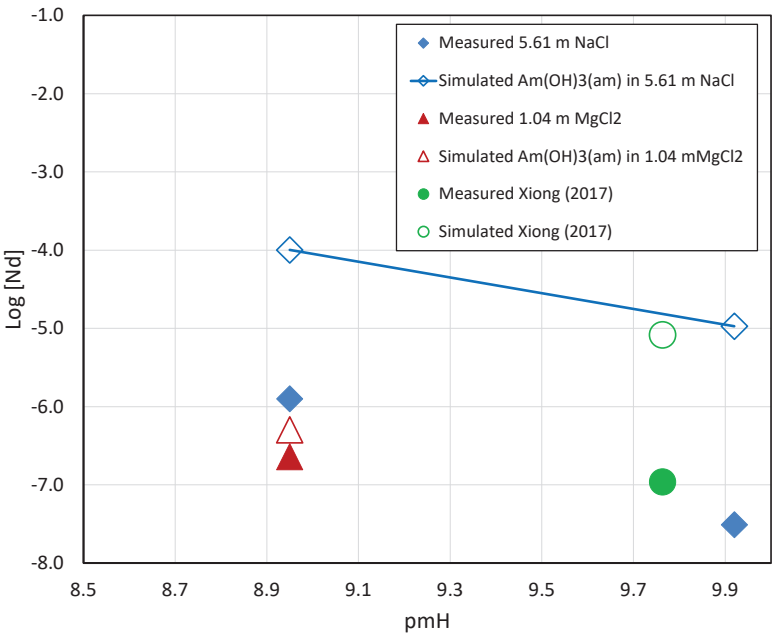


Figure A - 2. Graph of the Herm et al. (2015) and Xiong et al. (2017) measured data and EQ3NR model response using the DATA0.FM6 database with $Am(OH)_3(am)$ as the solubility-controlling phase.

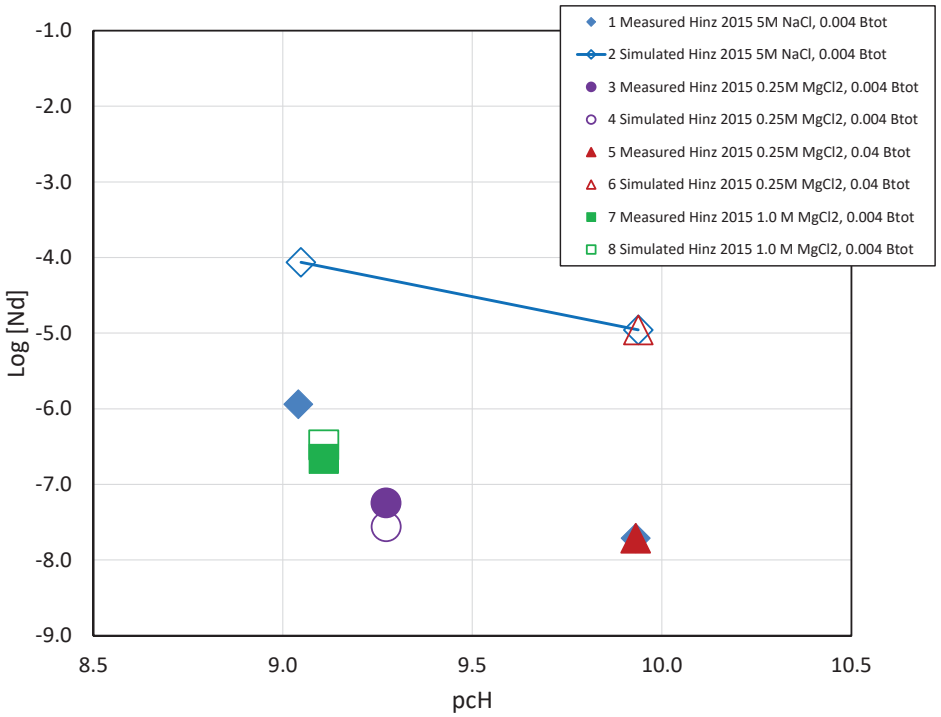


Figure A - 3. Graph of the Hinz et al. (2015) measured data and EQ3NR model response using the DATA0.FM6 database with $Am(OH)_3(am)$ as the solubility controlling phase.

Information Only

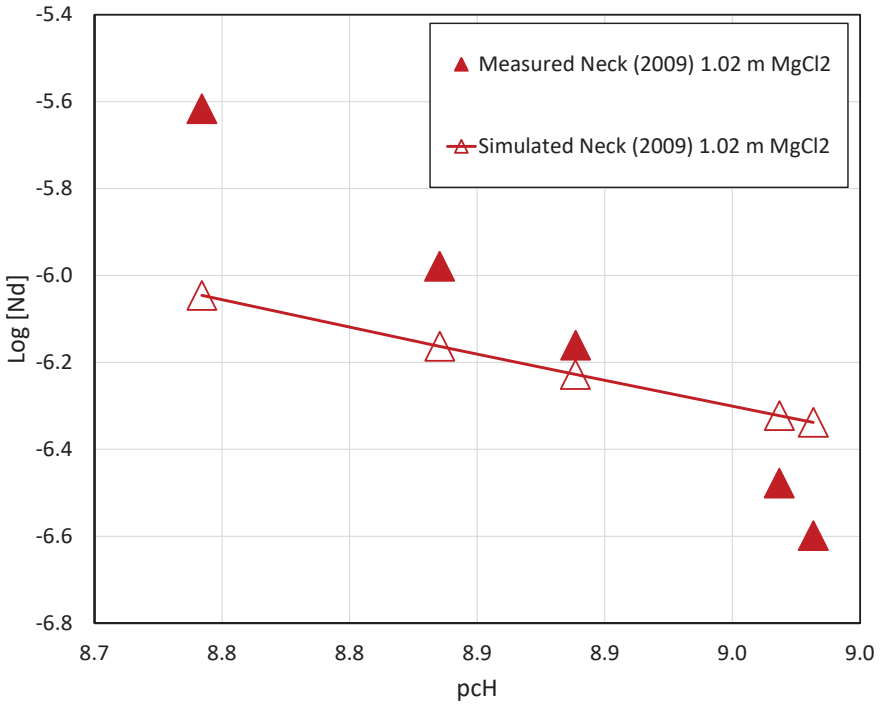


Figure A - 4. Graph of the Neck et al. (2009) measured data and EQ3NR model response using the DATA0.FM6 database with $Am(OH)_3(am)$ as the solubility controlling phase.

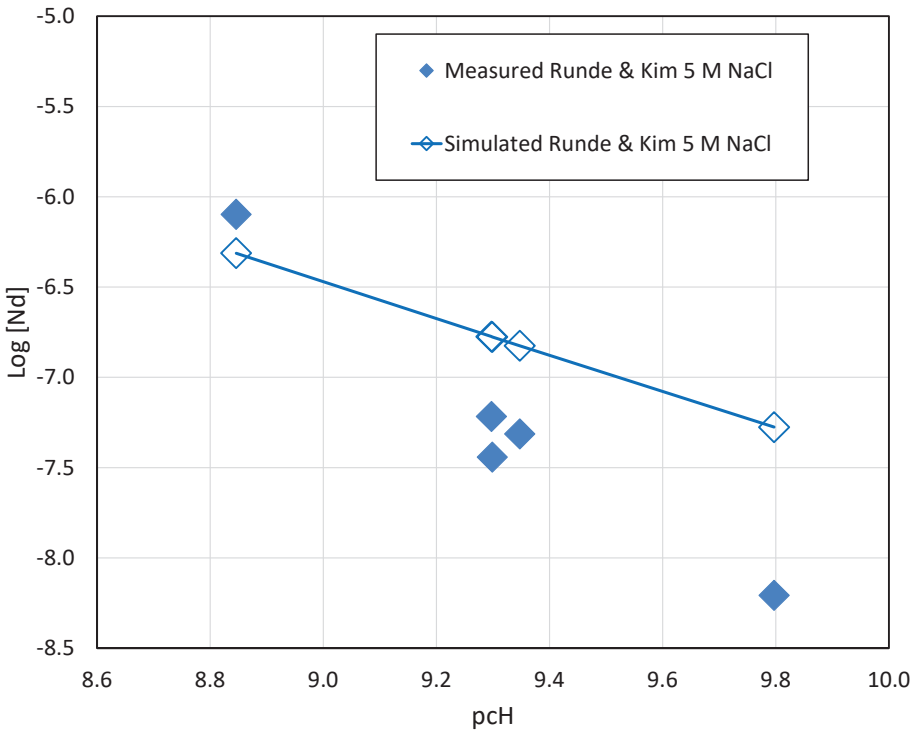


Figure A - 5. Graph of the Runde and Kim (1995) measured data and EQ3NR model response using the DATA0.FM6 database with $Am(OH)_3(s)$ as the solubility-controlling phase.

Information Only

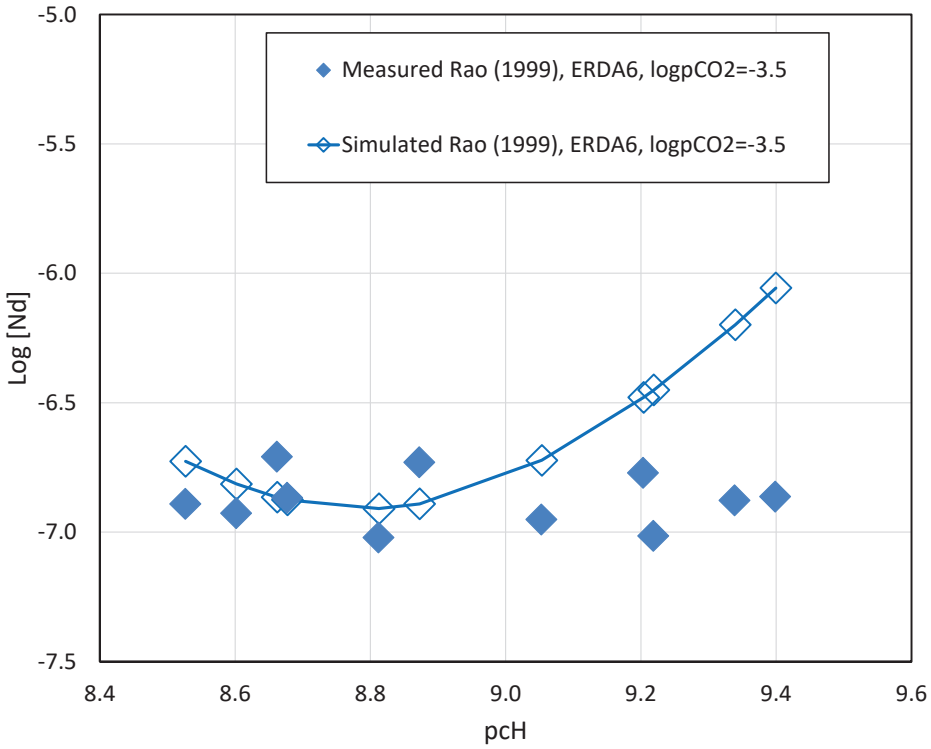


Figure A - 6. Graph of the Rao et al. (1999) measured data and EQ3NR model response using the DATA0.FM6 database with $NaAm(CO_3)_2.6H_2O(cr)$ as the solubility-controlling phase.

Information Only

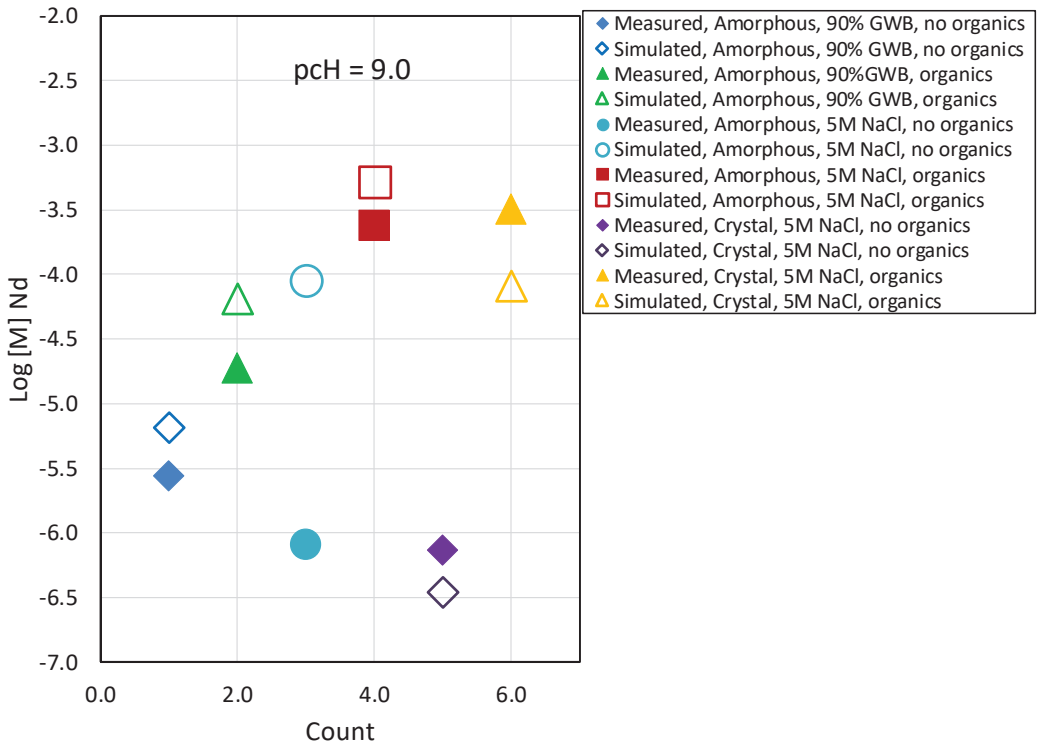


Figure A - 7 Graph of the Kutahyali Aslani (2022) measured data and EQ3NR model response using the DATA0.FM6 database with $Am(OH)_3$ (am) and $Am(OH)_3$ (cr) as the solubility-controlling phase at pcH = 9.0.

Results

Figures A – 1 – A – 7 show the WIPP model fits to the measured experimental data. Overall the visual fit of the WIPP model is subjectively fair compared to the measured data. By which it may be said that the WIPP model, both An(IV) and An(III), fits some data better than others, and taken as a whole, may be described, in the opinion of the author, as a "fair" overall fit to the experimental data.

Information Only

Appendix B. Kutahyali Aslani (2022) Dataset

Table B - 1 Provides the Nd(III) concentrations in molarity, the sample date, the matrix composition, and the sample pcH.

	pC_{H+} X-O-Am-7		pC_{H+}-X-Am-7
Elapsed Time (Days)	Concentrations of Nd^{3+} (M) in pC_{H+} 7 brine for amorphous solids with organics	Elapsed Time (Days)	Concentrations of Nd^{3+} (M) in pC_{H+} 7 brine for amorphous solids without organics
33	8.91E-05	33	1.87E-06
64	9.23E-05	64	2.15E-06
96	7.30E-05	96	1.46E-06
153	8.03E-05	153	1.29E-06
251	7.25E-05	251	1.33E-06
	pC_{H+} X-O-Am-9		pC_{H+} X-Am-9
Elapsed Time (Days)	Concentrations of Nd^{3+} (M) in pC_{H+} 9 brine for amorphous solids with organics	Elapsed Time (Days)	Concentrations of Nd^{3+} (M) in pC_{H+} 9 brine for amorphous solids without organics
33	1.40E-05	33	2.77E-06
64	1.86E-05	64	5.25E-06
96	2.05E-05	96	1.91E-06
153	2.08E-05	153	1.89E-06
251	2.03E-05	251	1.91E-06
	pCH+ X-O-Am-11		pCH+ X-Am-11
Elapsed Time (Days)	Concentrations of Nd^{3+} (M) in pC_{H+} 11 brine for amorphous solids with organics	Elapsed Time (Days)	Concentrations of Nd^{3+} (M) in pC_{H+} 11 brine for amorphous solids without organics
33	2.34E-05	33	3.45E-07
65	3.77E-05	65	2.27E-07
96	3.85E-05	96	1.59E-07
153	4.56E-05	153	1.76E-07
251	5.11E-05	251	1.01E-07

	01M NaCl-O-7		01M NaCl-7
Elapsed Time (Days)	Concentrations of Nd^{3+} (M) in 0.1 M NaCl, amorphous, pCH+ 7, with organics	Elapsed Time (Days)	Concentrations of Nd^{3+} (M) in 0.1 M NaCl, amorphous, pCH+ 7, without organics
32	4.13E-04	33	5.68E-05
64	5.54E-04	65	5.89E-05
95	5.91E-04	96	5.00E-05
159	6.41E-04	160	4.43E-05
263	7.55E-04	264	7.37E-05

Information Only

	01M NaCl-O-9		01M NaCl-9
Elapsed Time (Days)	Concentrations of Nd^{3+} (M) in 0.1 M NaCl, amorphous, pCH+ 9, with organics	Elapsed Time (Days)	Concentrations of Nd^{3+} (M) in 0.1 M NaCl, amorphous, pCH+ 9, without organics
32	2.40E-04	32	1.11E-07
64	3.26E-04	64	2.70E-07
95	3.43E-04	95	1.28E-07
159	3.51E-04	159	5.28E-08
263	4.44E-04	264	1.89E-06
	01M NaCl-O-11		01M NaCl-11
Elapsed Time (Days)	Concentrations of Nd^{3+} (M) in 0.1 M NaCl, amorphous, pCH+ 11, with organics	Elapsed Time (Days)	Concentrations of Nd^{3+} (M) in 0.1 M NaCl, amorphous, pCH+ 11, without organics
33	1.47E-04	33	8.40E-08
64	1.92E-04	64	1.33E-07
95	1.84E-04	95	1.83E-07
159	1.69E-04	159	7.54E-08
263	2.04E-04	263	4.17E-07
	5M NaCl-O-7		5M NaCl-7
Elapsed Time (Days)	Concentrations of Nd^{3+} (M) in 5 M NaCl, amorphous, pCH+ 7, with organics	Elapsed Time (Days)	Concentrations of Nd^{3+} (M) in 5 M NaCl, amorphous, pCH+ 7, without organics
32	2.03E-04	33	3.56E-05
63	3.15E-04	67	5.04E-05
94	3.73E-04	98	4.93E-05
158	4.39E-04	158	3.79E-05
262	5.32E-04	262	6.98E-05
	5M NaCl-O-9		5M NaCl-9
Elapsed Time (Days)	Concentrations of Nd^{3+} (M) in 5 M NaCl, amorphous, pCH+ 9, with organics	Elapsed Time (Days)	Concentrations of Nd^{3+} (M) in 5 M NaCl, amorphous, pCH+ 9, without organics
33	1.83E-04	30	4.90E-08
67	2.35E-04	64	2.62E-07
98	2.36E-04	95	1.12E-07
158	2.51E-04	155	1.35E-07
262	2.84E-04	259	3.58E-06
	5M NaCl-O-11		5M NaCl-11

Information Only

Elapsed Time (Days)	Concentrations of Nd^{3+} (M) in 5 M NaCl, amorphous, pCH+ 11, with organics	Elapsed Time (Days)	Concentrations of Nd^{3+} (M) in 5 M NaCl, amorphous, pCH+ 11, without organics
30	1.59E-04	30	3.51E-08
64	1.52E-04	64	8.82E-08
95	1.62E-04	98	1.79E-07
155	1.68E-04	155	1.83E-07
259	1.78E-04	259	1.75E-07

	01M NaCl-O-7		01M NaCl-7
Elapsed Time (Days)	Concentrations of Nd^{3+} (M) in 0.1 M NaCl, crystalline, pCH+ 7, with organics	Elapsed Time (Days)	Concentrations of Nd^{3+} (M) in 0.1 M NaCl, crystalline, pCH+ 7, without organics
29	9.75E-04	29	1.91E-04
63	1.08E-03	63	2.26E-04
97	1.10E-03	97	2.19E-04
155	1.11E-03	155	2.18E-04
259	1.15E-03	259	2.42E-04
	01M NaCl-O-9		01M NaCl-9
Elapsed Time (Days)	Concentrations of Nd^{3+} (M) in 0.1 M NaCl, crystalline, pCH+ 9, with organics	Elapsed Time (Days)	Concentrations of Nd^{3+} (M) in 0.1 M NaCl, crystalline, pCH+ 9, without organics
36	9.28E-04	36	2.34E-05
64	1.12E-03	64	5.68E-06
97	1.10E-03	97	5.85E-06
155	1.13E-03	155	2.95E-07
259	1.12E-03	259	1.62E-06
	01M NaCl-O-11		01M NaCl-11
Elapsed Time (Days)	Concentrations of Nd^{3+} (M) in 0.1 M NaCl, crystalline, pCH+ 11, with organics	Elapsed Time (Days)	Concentrations of Nd^{3+} (M) in 0.1 M NaCl, crystalline, pCH+ 11, without organics
35	5.26E-04	34	2.24E-08
63	7.74E-04	62	6.63E-08
96	7.93E-04	95	9.30E-08
154	8.84E-04	153	7.73E-08
258	1.06E-03	257	1.82E-07

	5M NaCl-O-7		5M NaCl-7
Elapsed Time (Days)	Concentrations of Nd^{3+} (M) in 5 M NaCl, crystalline, pCH+ 7, with organics	Elapsed Time (Days)	Concentrations of Nd^{3+} (M) in 5 M NaCl, crystalline, pCH+ 7, without organics
32	9.46E-04	32	7.05E-6
64	1.19E-03	64	1.27E-5

Information Only

93	1.23E-03	93	1.19E-5
149	1.36E-03	149	2.19E-5
253	1.25E-03	253	2.00E-5
	5M NaCl-O-9		**5M NaCl-9**
Elapsed Time (Days)	**Concentrations of Nd^{3+} (M) in 5 M NaCl, crystalline, pCH+ 9, with organics**	**Elapsed Time (Days)**	**Concentrations of Nd^{3+} (M) in 5 M NaCl, crystalline, pCH+ 9, without organics**
32	2.65E-4	35	4.04E-7
64	4.47E-4	66	2.09E-7
93	5.03E-4	98	8.02E-7
149	6.67E-4	149	4.62E-7
253	7.85E-4	253	9.43E-7
	5M NaCl-O-11		**5M NaCl-11**
Elapsed Time (Days)	**Concentrations of Nd^{3+} (M) in 5 M NaCl, crystalline, pCH+ 11, with organics**	**Elapsed Time (Days)**	**Concentrations of Nd^{3+} (M) in 5 M NaCl, crystalline, pCH+ 11, without organics**
34	2.21E-4	35	4.55E-7
65	3.19E-4	66	4.08E-7
97	2.96E-4	98	6.87E-7
148	3.51E-4	149	6.17E-7
252	4.22E-4	253	1.53E-6

Information Only